Journal of
Microscopy

Journal of Microscopy, Vol. 00, Issue 00 2016, pp. 1–11 doi: 10.1111/jmi.12477
Received 25 March 2016; accepted 26 August 2016

Survey: interpolation methods for whole slide image processing

L. ROSZKOWIAK*, A. KORZYNSKA*, J. ZAK*, D. PIJANOWSKA*, Z. SWIDERSKA-CHADAJ† & T. MARKIEWICZ†,‡

**Laboratory of Processing Systems of Microscopic Image Information, Nalecz Institute of Biocybernetics and Biomedical Engineering, Polish Academy of Sciences, Warsaw, Poland*

†Institute of Theory of Electrical Engineering, Measurement and Information Systems, Faculty of Electrical Engineering, Warsaw University of Technology, Warsaw, Poland

‡Department of Pathology, Military Institute of Medicine, Szaserow, Warsaw, Poland

Key words. Biomedical engineering, image interpolation, image processing, microscopic images, whole slide images.

Summary

Evaluating whole slide images of histological and cytological samples is used in pathology for diagnostics, grading and prognosis . It is often necessary to rescale whole slide images of a very large size. Image resizing is one of the most common applications of interpolation. We collect the advantages and drawbacks of nine interpolation methods, and as a result of our analysis, we try to select one interpolation method as the preferred solution. To compare the performance of interpolation methods, test images were scaled and then rescaled to the original size using the same algorithm. The modified image was compared to the original image in various aspects. The time needed for calculations and results of quantification performance on modified images were also compared. For evaluation purposes, we used four general test images and 12 specialized biological immunohistochemically stained tissue sample images. The purpose of this survey is to determine which method of interpolation is the best to resize whole slide images, so they can be further processed using quantification methods. As a result, the interpolation method has to be selected depending on the task involving whole slide images.

Introduction

Interpolation is a well-known method of estimation of values of data between two known values. Fundamentally, interpolation changes the image from a discrete matrix of samples into a continuous image. The basis to perform the interpolation is the hypothesis that data are continuous and can be defined at any given point. The scope of use for interpolation is extensive: from basic one-dimensional (1D) signal interpolation, to 2D and 3D data-like images or stacks of images. Whenever it is required to get the value between two discrete samples of data, interpolation is used.

The most common 2D signal for interpolation is image. Interpolation is often used during a preprocessing stage of the more complicated process. Also, it is a part of complex algorithms, commonly used in image processing. Some of its uses are geometric operations, resizing, compression, correction of spatial distortion, image decomposition and is crucial to subpixel image registration. Simple geometric operations such as rotation, translation and scaling often need subpixel coordinates.

Interpolation is crucial for tasks like medical image processing. For example, use of inverse Radon transform requires interpolation in computer tomography and in magnetic resonance imaging for image reconstruction, and fitting one set of data to the other for multimodal imaging. Changing the aspect ratio is sometimes necessary when the scanner (or other device) does not have a homogenous resolution of charge-coupled device (CCD) sensor (and frame grabber) to acquire pictures (Lehmann *et al.*, 1999). To preserve the true aspect ratio, interpolation has to be used. Cameras also use the interpolation with Bayer filter to perform demosaicing, which yields a typical colour image.

One of the most popular applications of interpolation is image resizing. It can be used to rescale and resample the image. Zooming and scaling are not to be confused (Sellaro *et al.*, 2013), because zooming does not need image resampling. That is why the role of image interpolation is so vital while evaluating whole slide images (WSI) (Korzynska *et al.*, 2010; Slodkowska *et al.*, 2011; Neuman *et al.*, 2013) of histological (Bueno *et al.*, 2012; Korzynska *et al.*, 2014; Lopez *et al.*, 2014) and cytological (Markiewicz *et al.*, 2009; Rojo *et al.*, 2010; Callau *et al.*, 2015) samples. Since those are images enormous in size, it is often necessary to lower their resolution or rescale them.

Digital images resizing is the main problem in this paper, and it concerns certain types of images: immunohistochemically

Correspondence to: Lukasz Roszkowiak, Nalecz Institute of Biocybernetics and Biomedical Engineering, Ks. Trojdena 4 Str., Warsaw, Poland. Tel: +48-22-659-9143 (ext. 124); fax: +48-22-659-7030; e-mail: lroszkowiak@ibib.waw.pl

stained tissue samples images. These types of images are collected and quantified using internet platform MIAP (Markiewicz, 2011; Swiderska *et al.*, 2015; Markiewicz, 2016) for pathologists, researchers and students. To achieve comparability of the results with an automated computer-aided quantification method implemented on the MIAP, the images and WSI from various acquisition tools uploaded by users should be unified in pixel size.

The immunohistochemically stained tissue sample images vary in size and pixel size depending on the acquisition devices. A significant aspect is the quality characteristics inherited by the basis interpolation function. A survey is used to choose an interpolation method that preserves image features important for quantification methods and is suitable to implement a parallel function to achieve decrease of time of large-size images processing.

Image interpolation is nowadays commonly implemented in most image processing programs like Photoshop and Corel (commercial) or Gimp and ImageJ (freeware). Most often, we have a very limited number of methods available, or no choice of methods at all. So it was decided to compare some known methods and evaluate them on a set of standard images known in image processing and on a set of the immunohistochemically stained tissue samples images.

In this survey, we try to answer the following question: 'Which is the best method of interpolation to process whole slide images to be further processed using quantification methods based on colour, texture, objects size and shape?'

Image artefacts introduced by interpolation. Errors introduced in an image are undesired alterations in pixel values, called artefacts. Many artefacts were named after the visual effect that can be observed in result image such as blurring, aliasing, ringing, blocking and colour distortion (Thevenaz *et al.*, 2000). Each type of artefact has different effect on the image characteristics relevant to quantification methods that are based on the colour, size, shape and texture. Examples of artefacts are presented in Figure 1.

Blurring causes a mismatch between the original image and the interpolated image. It can occur after downsampling as well as oversampling. The interpolated image is smoother than the original, and appears to be out of focus. The shape is kept, but the texture and coarseness (especially of the object's borders) is lost (see Figure 1B). Analysing blurred images with quantification methods results in objects extended in size and with changed texture; the latter is critical to identify objects of interest.

Aliasing often occurs simultaneously with blurring. It is one of the main problems with downsampling. It causes two different signals (objects) to become indistinguishable after interpolation. While downsampling, it is not always possible to keep the coarseness with less samples, and it is impossible to return to the original state of the image. When aliasing is present in the image, we can observe it as a moiré effect and less frequently as texture. The quantification methods, which analyse images with aliasing, tend to have incorrect (decreased) number of found objects of interest.

Blocking is the problem of piece-wise interpolation methods, generally when the interpolant is finite. Since interpolation can be evaluated for a limited amount of data, it is visible in the outcome as blocks. It is especially visible in the nearest neighbour algorithm (see Figure 1C). As blocking strongly influences texture, it causes problems for the quantification methods.

Ringing is most visible near sharp edges. It happens when the interpolation functions are oscillating. While interpolating with subpixel lengths in spectral domain, it tries to represent the image as a sum of smooth oscillating waves. This is strongly connected with the Gibbs effect. Sometimes it is possible to recover the original image even when there are a lot of visible ringing effects present in the interpolated image. Unfortunately, this strongly affects the results of the quantification methods in images with ringing as oscillating waves distort shape size and texture (see Figure 1D).

Colour distortion: While interpolating images in red, green and blue (RGB) colour space, the values representing colour are changed. For medical application of the quantification methods, the colour information is so important that any changes are forbidden.

Interpolation methods

Nearest neighbour. It is the most simple, nonadaptive, method of interpolation (Jain, 1989). The nearest neighbour algorithm is very simple to implement and is commonly used. As this method copies available values and does not introduce new values to the data, it is not technically an interpolation method. The nearest neighbour algorithm is based on the distance between data points. This algorithm treats the image as a grid with values of pixels on grid nodes. Then, the position of the interpolated (new) pixel is overlaid on the original image, and the distances between the new pixel and its neighbouring points are calculated. The value of nearest point to each grid node of new image is assigned.

$$f(x) = \begin{cases} 1 & \text{for } 0 \leq |x| < 0.5 \\ 0 & otherwise. \end{cases} \quad (1)$$

Linear/bilinear. If the coordinates of two data points are known, the linear interpolant is the straight line between these points. In this method, both neighbouring points influence the value of interpolated data point (new pixel value). The values are weighted by their distance to the interpolated point.

Bilinear interpolation method (Meijering, 2002) is an extension of linear interpolation method for 2D variables, such as images. For bilinear interpolation four pixels are taken into

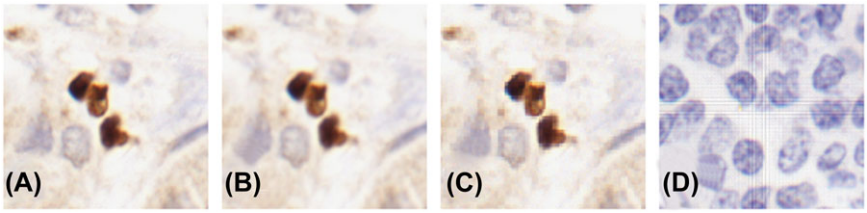

Fig. 1. Typical artefacts introduced by downsampling and upsampling interpolation methods on images of tissue sample stained immunohistochemically with 3,3'-Diaminobenzidine (DAB) and haematoxylin. (A) Unprocessed image fragment; (B) same fragment from A with blurring introduced by bilinear method (scale 0.8); (C) same fragment from A with blocking introduced by nearest neighbour algorithm; and (D) fragment of whole slide images (WSI) with visible oscillation on tile border.

account. Direct neighbours in both directions influence the value depending on the distance. The closer they are, the greater effect.

$$f(x) = \begin{cases} 1 - |x| & \text{for } 0 \leq |x| < 1 \\ 0 & otherwise. \end{cases} \quad (2)$$

Bicubic. Compared with bilinear interpolation algorithm, bicubic interpolation algorithm (Keys, 1981) extends the influence using more points. To calculate the value of interpolated pixel, values of 16 adjacent pixels are weighted according to their distance to the analysed pixel.

$$f(x) = \begin{cases} \frac{3}{2}|x|^3 - \frac{5}{2}|x|^2 + 1 & for\ 0 \leq |x| < 1 \\ -\frac{1}{2}|x|^3 + \frac{5}{2}|x|^2 - 4|x| + 2 & for\ 1 \leq |x| < 2 \\ 0 & otherwise. \end{cases} \quad (3)$$

Cosine. This method is similar to linear interpolation. A smoother interpolating function is often desirable, so instead of linear function it uses cosine function (Scheiber, 2011). Between two points with known values and coordinates the interpolant is a line defined by cosine function. Cosine function provides a more smooth transition between points.

$$f(x) = x_1 + \frac{1 - cos(pi * T)}{2} * (y_2 - y_1). \quad (4)$$

Sinc. The sinc function is defined by $sinc(x) = sin(x)/x$ where $x \neq 0$ and $sinc(0) = 1$. The sinc interpolation formula is

$$f(x) = \sum_{n=-\infty}^{\infty} f_n sinc\left(\frac{\pi}{T}(x - nT)\right), \quad (5)$$

where T is the sampling period, f_n original signal and $f(x)$ is interpolated signal. This is a representation of linear convolution between the signal f_n with scaled and shifted samples of the sinc function. Sinc (Meijering *et al.*, 1999) filter is an 'ideal' low-pass filter in the frequency sense. It is an idealized filter that removes all frequency components above a given cutoff frequency, and allows the perfect passing of low frequencies. Sinc function is the theoretically optimal kernel for convolution-based interpolation of originally band-limited images. Real examples have finite spatial support, and it is not possible for the sampling frequencies to satisfy the Nyquist criterion. Consequently, it is impossible to retrieve the original images exactly from the resulting samples by means of sinc interpolation. Additionally, it cannot be computed in practice, except in the case of periodic images, which are not likely to occur in medical imaging (Meijering *et al.*, 2001). A frequently used approach to obtain a sinc-approximating kernel is modelling the shape of the sinc kernel by piecewise polynomials.

b-splines. Splines are used to describe a curve by mathematical means. Representation is based on a series of points at specified intervals and by a function. Consequently, this allows calculating position of additional points within an interval. B-spline (Hou & Andrews, 1978; Unser *et al.*, 1991) is short for basis spline, and the points on which spline is set are called control points. Valuable feature is that spline curves are continuous at the control points.

$$f(x) = \sum_{k=-\infty}^{+\infty} B_{k,n+1}(x) \bullet f(x_k). \quad (6)$$

Hermite. This method uses spline in Hermite form (Spitzbart, 1960). It requires values of four known points, to produce higher degree of continuity. Each piece is a third degree polynomial specified by values of the points and first derivatives at the end points. As a result the spline, as well as its first derivative, is continuous. Hermite interpolation keeps the monotonicity of the original data. That means the original and interpolated data points have local extrema at the same positions.

$$f(x) = \sum_{i=0}^{N} f(x_i) {h_i}^{(0)}(x) + \sum_{i=0}^{N} f'(x_i) {h_i}^{(1)}(x). \quad (7)$$

Lagrange. This method finds a polynomial function that is defined by the Lagrange interpolating polynomial (Rowland, 1979). The polynomial must pass through several control points, which can be specified. It this paper, we use four and six control points. The passband characteristics are improved

by raising the order (the number of control points) of the Lagrange kernel.

$$f_{Lagrange_4}(x) = \begin{cases} \frac{1}{2}|x|^3 - |x|^2 - \frac{1}{2}|x| + 1 & for\ 0 \le |x| < 1 \\ -\frac{1}{6}|x|^3 + |x|^2 - \frac{11}{6}|x| + 1 & for\ 1 \le |x| < 2 \\ 0 & otherwise. \end{cases} \quad (8)$$

Catmull-Rom splines. This method is based on splines (Twigg, 2003; Yuksel *et al.*, 2009). To calculate a point on the curve, two points on either side of the desired point are required. One of the distinctive characteristics of this method is the created curve passing through all of the control points. Generally, the created spline consists of continuous segments. The first derivatives of created curve are continuous. The second derivative is linearly interpolated within each segment, causing the curvature to vary linearly over the length of the segment.

$$f(x) = \frac{1}{6}\begin{cases} 9|x|^3 - 15x^2 + 6 & for\ |x| < 1 \\ -3|x|^3 + 15x^2 - 24|x| + 12 & for\ 1 \le |x| < 2 \\ 0 & otherwise. \end{cases} \quad (9)$$

Moreover, two additional methods were considered. Interpolation by quadratic polynomial equation (Schafer & Rabiner, 1973; Dodgson, 1997) and interpolation developed by Mitchell–Netravali (Mitchell & Netravali, 1988), which are based on parameterized cubic filters. It was believed that it keeps equilibrium between sharpness and smoothness resulting in superior image quality. Both methods were only used for theoretical considerations. We decided to exclude them from this evaluation due to an extremely long processing time.

Evaluation

To compare the performance of interpolation methods, test images were scaled and then rescaled to their original size with the same algorithm. The modified image was compared to the original image in various aspects. The time needed for calculations and results of quantification performance on modified images were also compared. All tested algorithms were developed in MATLAB R2015b implemented on Intel(R) Core(TM) i7-4710MQ @2.50 GHz CPU, 16.0 GB RAM.

Image evaluation

The mean squared error (MSE) is the most simple and widely used technique. It can be calculated by averaging the squared intensity differences of reference image and after interpolation image pixels. This method of evaluation is quite simple to calculate and has a clear interpretation. However, it is quite incomparable to human perception.

$$MSE = \frac{1}{mn}\sum_{i=0}^{m-1}\sum_{j=0}^{n-1}[I(i,\ j) - K(i,\ j)]^2. \quad (10)$$

Peak signal-to-noise ratio method (PSNR) (Huynh-Thu & Ghanbari, 2008) is the ratio between the maximum possible value of pixel and the value of noise that corrupts the fidelity in comparison to the original image. This feature is related to MSE as it is used in the calculations as a measure of noise. Typical values for the PSNR in lossy image and video compression are between 30 and 50 dB, provided the bit depth is 8 bits, where higher is better (Welstead, 1999; Hamzaoui & Saupe, 2006). This type of evaluation is also quite simple to calculate and has a clear interpretation, but it does not match human perception.

$$PSNR = 20log_{10}(MAX_{Int}) - 10log_{10}(MSE), \quad (11)$$

where MAX_{Int} is the maximum possible pixel value of the image.

Another measure is structural similarity (SSIM) (Wang *et al.*, 2004; Rouse & Hemami, 2008). It is matched to perceived visual quality, as image interpretation is performed using the perception-based model. The SSIM is a quality measure of reference image with perfect quality to interpolated image with distortions. As MSE and PSNR give absolute errors, the SSIM is a perception-based model. The degrading of the image is treated as perceived change in structural information also taking into consideration occurrence of luminance masking and contrast masking:

$$SSIM(x,\ y) = \frac{(2\mu_x\mu_y + c_1)(2\sigma_{xy} + c_2)}{\left(\mu_x^2 + \mu_y^2 + c_1\right)\left(\sigma_x^2 + \sigma_y^2 + c_2\right)}. \quad (12)$$

Evaluation dataset

For evaluation purposes, we used four general test images and 12 specialized biological tissue sample images used in pathology diagnostics, grading and prognosis. The general test group consists of (1) well-known standard test image 'Lenna' (in colour); (2) Indian head (Kay, 1949) (black and white) test pattern used from 1940 to make adjustments on cameras and monitors; (3) typical PAL colour test pattern (PM5544) used for calibration; (4) multiburst test pattern used to establish the frequency response of a video system. The biological image group consists of 12 images of breast cancer tissue received from Molecular Biology and Research Section, Hospital de Tortosa Verge de la Cinta, Institut d'Investigacio Sanitaria Pere Virgili (IISPV), URV, Spain, and Pathology Department of the same hospital. These images are cropped (to squares of 1000 pixels) fragments randomly selected from the bigger set of experimental images captured during previous investigation (Korzynska *et al.*, 2013). Images were cropped to achieve relatively fast evaluation. Tissue presented in the images varies from very dark to light and with sparse and compact architecture of cells. All images are focused and the qualities of the images are typical for this type of biological data.

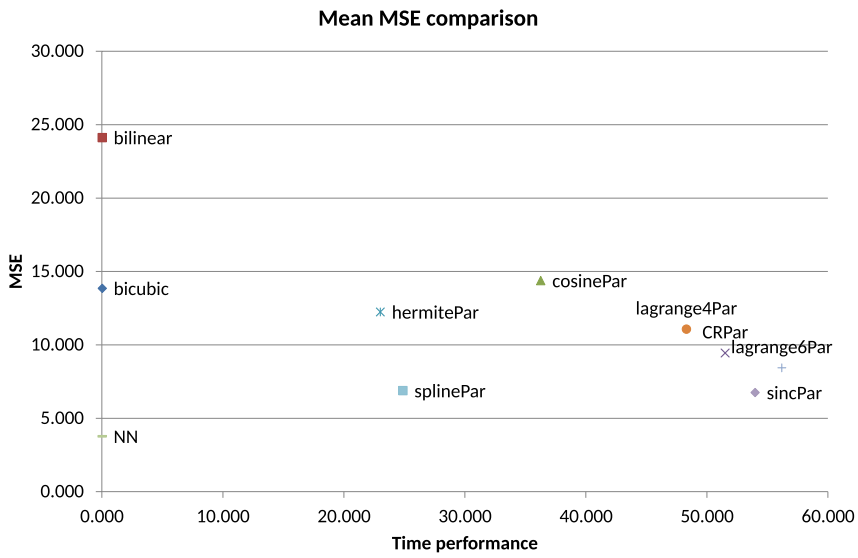

Fig. 2. Comparison of mean mean squared error (MSE) estimator with mean time elapsed during calculations for tested interpolation methods.

Runtime evaluation

The main problem of interpolation is computation time. Unfortunately, to achieve better results, the calculations require more time. For this reason, it is very important to find the best bias between acceptable results achieved in considerable amount of time. A significant aspect is the quality characteristics inherited by the basis interpolation function. The useful feature of interpolation method is separability. It is easier to use parallel computing when the calculation can be done line-by-line and column-by-column.

Quantification performance evaluation

We tried to evaluate the influence of the interpolation methods on the results of automated computer-aided quantification methods. This comparison was based on the number of cells segmented from the tissue images after interpolation processing in comparison with segmentation on original image. We used two methods developed previously by our research team; *method1* published previously (Neuman *et al.*, 2010) and *method2*, a recent method called Metinus (Roszkowiak *et al.*, 2016).

Results

We compared the means of MSE for 10 different resizing scales varied from 0.5 to 2. Mean errors are showed in comparison to mean time elapsed during calculations, as seen in Figure 2. From this comparison, we can assume that the nearest neighbour algorithm performs the best and the bilinear the worst, in the sense of mean distance between each pair of pixels in original and processed images. Spline and sinc methods perform acceptably well. The rest of methods are clustered with similar performance. The difference is in time consumed; bilinear, bicubic and nearest neighbour algorithms need fundamentally less time than the others. The reason is that these three methods are internal MATLAB function optimized by the developers. Among these other methods, the Hermite and spline methods are faster than cosine or Lagrange methods whereas Catmull-Rom and sinc methods are the most time consuming.

Next, similarly to MSE, we compared mean PSNR to time of evaluation as seen in Figure 3. The nearest neighbour is a very quick method with the lowest error values. The second best is the sinc method, but it is one of the slower methods. Unfortunately, both of those methods are not stable as they give very different results depending on the upscaling or downscaling. This effect can also be observed for SSIM evaluator, see Figure 4. Above the threshold of 40 dB, we have a cluster of very similar performance with different speed consisting of spline, cosine, Lagrange and Catmull–Rom methods.

A similar comparison was done for SSIM estimator. The spline method has the greatest similarity, whereas Lagrange, Catmull–Rom and Hermite methods also produce images very similar to the original. The nearest neighbour and sinc methods have very good performances, whereas interpolated image is bigger than the original but suffers losses with scale below one. Comparison of mean SSIM estimator with mean time elapsed during calculations is presented in Figure 4. Based on this comparison, we can assume that the best method is spline and the second best is Lagrange interpolation method.

The comparison of runtime performance is presented in Figures 2–4. In Figure 5, methods are ranked from fastest to slowest depending on overall mean of 10 different scale values. The first three methods that have original implementation in MATLAB are definitely the fastest. We tried to keep a similar implementation procedure for the rest of the methods so the times of computation are comparable.

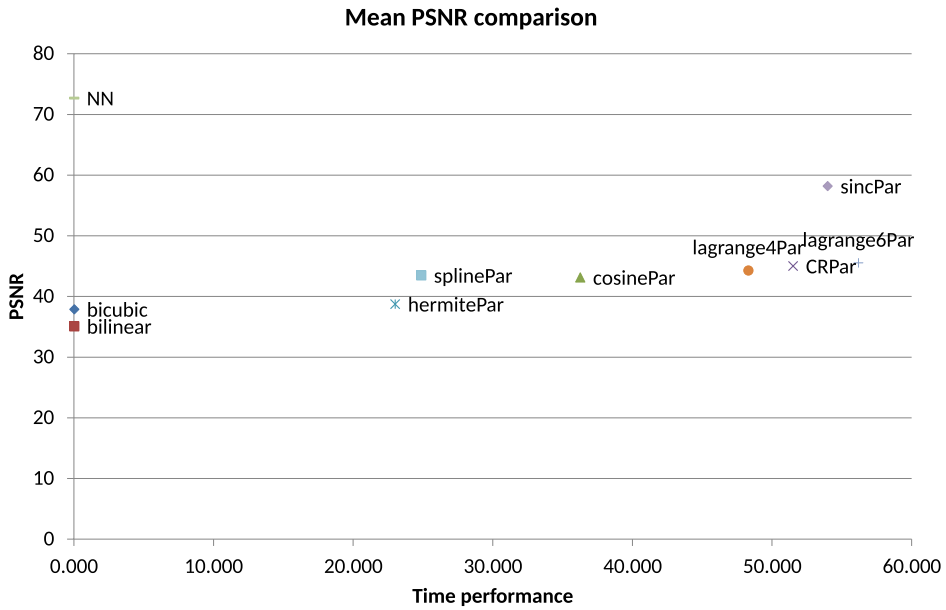

Fig. 3. Comparison of mean peak signal-to-noise ratio method (PSNR) estimator with mean time elapsed during calculations for tested interpolation methods.

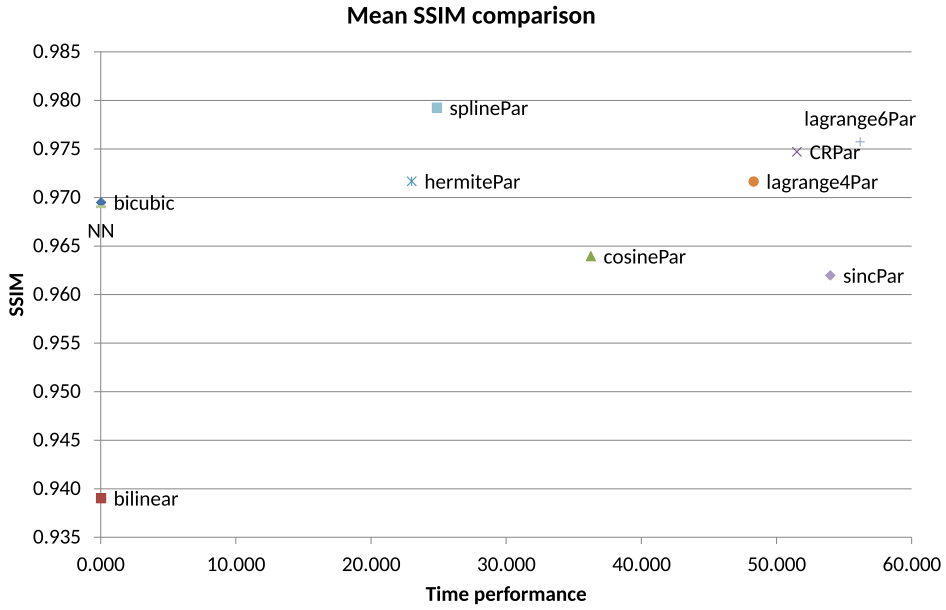

Fig. 4. Comparison of mean structural similarity (SSIM) estimator with mean time elapsed during calculations for tested interpolation methods.

The last comparison was based on the quantification results of the tissue images after interpolation processing in comparison with quantification of original images. In Table 1, we present the mean of difference between the number of objects found in original image and number of objects found in the image after rescaling with particular interpolation algorithm. We used two methods developed previously by our research team; *method1* published previously (Neuman *et al.*, 2010) and *method2*, a recent method called Metinus (Roszkowiak *et al.*, 2016). Both methods are based on selection of brown objects of interest according to colour, then segmenting the area of object based on size, texture and shape criteria. According to results presented in Table 1, all methods influence the possibility of identification of objects of interest using segmentation techniques. Based on this comparison, nearest neighbour and sinc methods give the best results, followed by Lagrange, Catmull-Rom and spline methods.

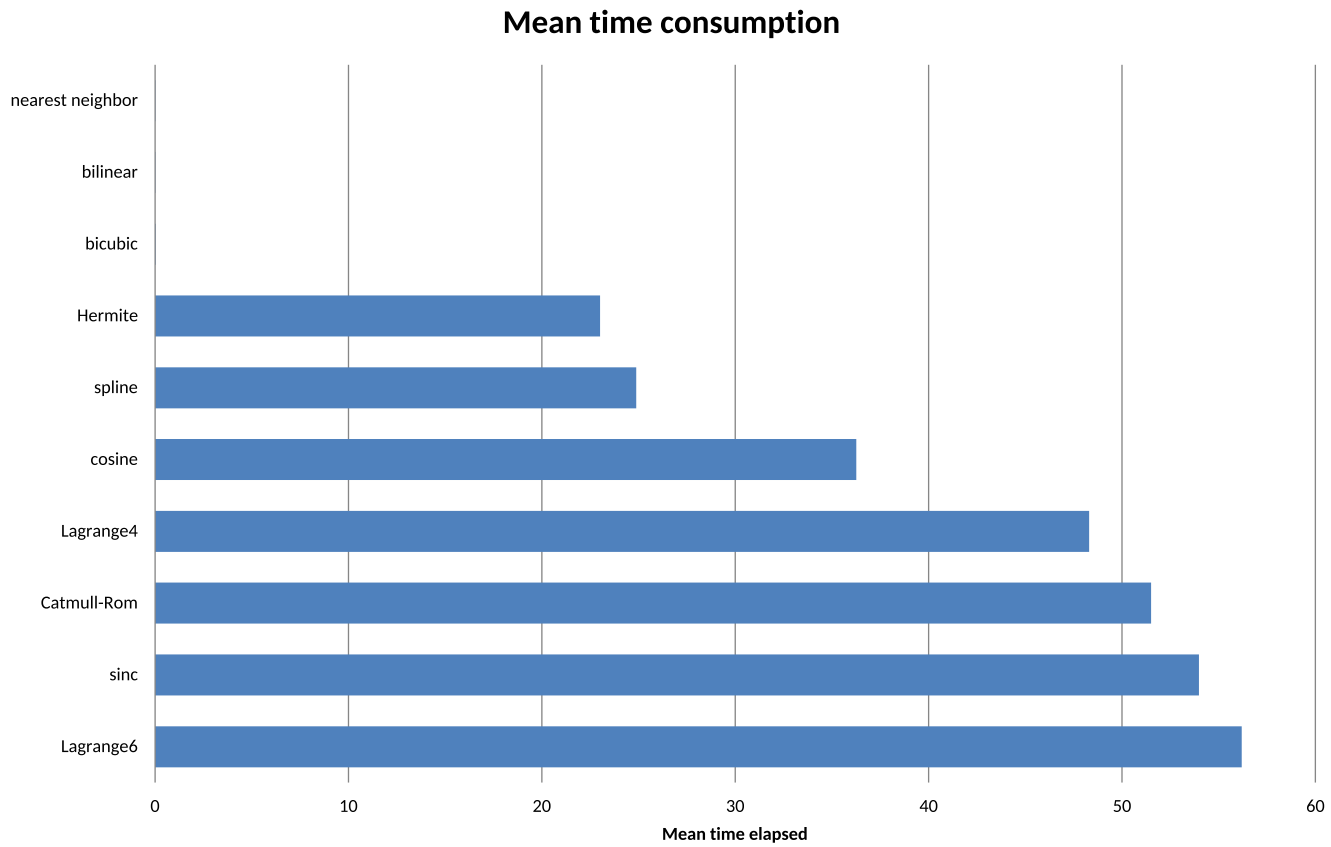

Fig. 5. Comparison of mean runtime performance calculated for 1000 × 1000 pixel size images. Presented as ranking from fastest to slowest method.

Table 1. Object segmentation comparison for two methods of segmentation. Mean and standard deviation of difference between objects found in original image and number of objects found in image after rescaling with interpolation algorithm (mean diff. = mean difference; std. dev. = standard deviation).

	method1		method2	
	Mean diff.	Std. dev.	Mean diff.	Std. dev.
Nearest neighbor	0.361	1.577	–0.083	0.989
Bilinear	0.653	2.314	3.986	5.285
Bicubic	0.139	1.833	1.472	2.162
Cosine	0.417	1.919	2.236	3.204
Sinc	0.194	1.562	0.097	0.808
Spline	0.292	1.533	0.625	1.261
Hermite	0.292	1.788	1.569	2.337
Lagrange_4	0.151	1.604	1.027	2.075
Lagrange_6	0.264	1.565	0.514	1.547
Catmull–Rom	0.139	1.577	0.903	1.770

Discussion

In this section, methods of interpolation are presented in the order of increasing usefulness for the resizing of the immunohistochemically stained tissue sample images before quantification.

The nearest neighbour interpolation algorithm is the simplest and extremely fast algorithm. It does not introduce new values to the interpolated image, so it preserves the original noise distribution. Unfortunately, this method does not have subpixel accuracy, so it often generates strong discontinuities (distortions) that can be observed as mosaic and saw tooth effects. Furthermore, the maintenance of texture is quite poor. The quality of interpolation result is not scale independent, and this method is applicable for upscaling rather than downscaling. All in all, it has very few advantages apart from great speed, so we can recommend it for upscaling of parts of images that do not include any vital information, that is, vast background.

A more complex method is the bilinear interpolation. The calculations are performed in a continuous manner, so there are no discontinuity flaws like in the nearest neighbour. This method works similar to low pass filter, so that the high-frequency component (edges and details in image) is reduced and contours become blurry. Another disadvantage is the aliasing beyond the low frequencies cutoff point. This effect can be observed as poor evaluation results, specifically higher MSE and lower SSIM. Also, the number of segmented objects

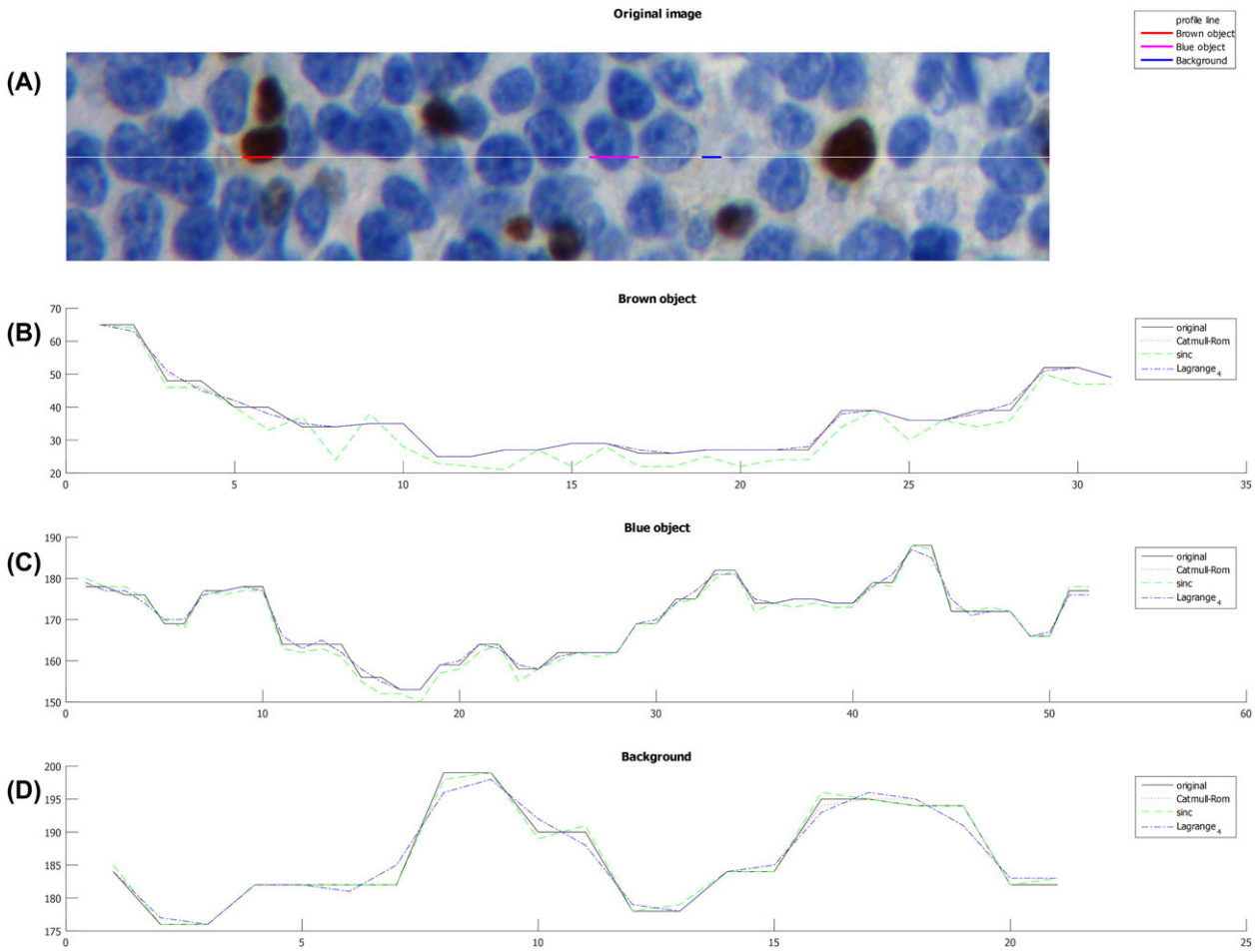

Fig. 6. Comparison of interpolation performance. Comparison is performed for brown (B) and blue (C) object and background (D) fragment, marked by colour segments on the white profile line (A). Original values (black line) are compared with values after interpolation performed with recommended functions: Catmull–Rom (red dotted line), sinc (green dashed line) and Langrange (blue dash-dot line). For clarity only blue channel (of RGB) is showed. Interpolation scale: 0.9.

in images rescaled with bilinear algorithm is the most different from the original. Because the complexity of calculation is higher, this method is also slower than nearest neighbour algorithm. Because of all the disadvantages, this method is not recommended.

Next on the complexity ranking is the bicubic interpolation. This method needs even more computation than the two previous methods. Bicubic method gives average results for all three estimators. Alas, the segmentation of image rescaled using bicubic method results in quite high variability of found objects (see Table 1) mostly because of its tendency to blurring. Although this method is considered to be a fine compromise between speed and satisfactory results and is most commonly used in many popular image processing software, it is not recommended to be used with immunohistochemically stained tissue sample images.

In general, the idea to use spline interpolation is to increase smoothness of the result image. Since this method is working as a low pass filter, the edges are visibly smooth but a little blurred. There are no instances of saw tooth phenomenon while using this method. The main disadvantage is that the interpolated curve may not pass through the original control points, which results in changes in colour for RGB images. According to MSE and SSIM evaluators spline method gives good results. As for PSNR, it gives an average result in comparison to other methods. It is also one of the relatively fast methods, but still it is not recommended for the WSI interpolation mainly because of its relatively large standard deviation in results of quantification.

Using cosine function as an interpolant removes the problem of discontinuities, therefore giving slightly better results in comparison to linear interpolation, with average evaluation errors. The number of segmented objects in images rescaled with cosine algorithm differ significantly from the original. Because of that, this method is not recommended for the WSI interpolation.

The Hermite interpolation gives average results according to all three estimators, and it is also a relatively fast method. Smoothing the interpolated image causes losses in texture what may be disastrous for some further processing methods. High standard deviation of the number of found objects of interest can be observed in Table 1, and causes this method to be not recommended.

Catmull–Rom is similar to Hermite interpolation, but the points along the original set of points are also present in the spline curve. The created curvature may not be continuous in second derivatives. This results in quite crisp interpolated images. To sum up, Catmull–Rom interpolation yields passable results with acceptable time of computation, and it can be recommended for the use on immunohistochemically stained tissue sample images.

Sinc interpolation function is an optimal interpolator for band-limited data, and some properties can be derived from this function. This method tries to avoid smoothing the image and preserves high frequencies. Based on MSE and PSNR, it gives very good results. However, the low value of SSIM parameter suggests that for human observation it might seem as a worse interpolator than other methods. Moreover, sinc interpolation is one of the slowest tested methods. This method produces very little variability in the number of segmented objects of interest. Interestingly, interpolating WSI images gives strong oscillations in the output, probably where tile borders of WSI are located. But, it seems they do not disturb quantification as can be observed in Table 1. This method is recommended to be used but only if there is no time limit.

Lagrange polynomial method has more complicated formula than other polynomial methods. It does not need evenly spaced values to interpolate, but it may cause oscillation, similarly to other methods that use polynomial while interpolating data with equally spaced points. This oscillation above and below the true function may grow with a number of control points. We tried to eliminate this problem by reducing the number of control points to 4 and 6, which causes oscillations on the level that do not disturb quantification methods. This method gives good results judging by MSE and SSIM. Also, the number of elements is consistent with the use of segmentation algorithms (see Table 1). Lagrange polynomial based method of interpolation is strongly recommended to resize images before quantification if resizing is needed.

Conclusion

In the Introduction section we stated a question: 'Which method of interpolation is the best to rescale WSI to be further processed using quantification methods based on colour, texture, objects size and shape?', which we tried to answer with this survey. Based on the results of comparison we can say that there is no one method that can be ultimately used for every purpose. Interpolation method has to be selected for every task involving WSI, separately, to fit specific image quantification method.

Based on this study, the sinc, Catmull–Rom and Lagrange interpolation methods have been chosen for resizing of images and WSI coming from various acquisition tools. In Figure 6, fragments of images after interpolation with selected methods are presented. It seems that all interpolation methods that introduce any low frequency filtration are rejected, as they disturb objects colour and texture as well as its size and shape.

If the need for interpolation of whole WSI for coarse inspection arises, then we suggest using nearest neighbour algorithm, as it is the fastest. WSI is often divided into smaller regions of interest for purpose of image processing. It is then possible to use slower method of interpolation, which gives better results. In this case, we propose the use of Lagrange polynomial interpolation. If regions of interest partly consist of background, this part can be interpolated quickly without worrying about information loss with the nearest neighbour algorithm.

In the future work, we plan to optimize selected methods of interpolation to make them work faster without a loss of performance. Moreover, we would like to verify if the results of this study comply with other types of staining, like haematoxylin–eosin standard stain and tissue where membrane or cytoplasm instead of nuclei is stained.

Acknowledgements

This study was supported by the National Centre for Research and Development (Narodowe Centrum Badan i Rozwoju), Poland (grant PBS2/A9/21/2013).

We would like to thank Molecular Biology and Research Section, Hospital de Tortosa Verge de la Cinta, Institut d'Investigacio Sanitaria Pere Virgili (IISPV), URV, Spain, and Pathology Department of the same hospital for a longtime cooperation and sharing of samples.

References

Bueno, G., Gonzalez, R., Deniz, O., Garcia-Rojo, M., Gonzalez-Garcia, J., Fernandez-Carrobles, M., Vallez, N. & Salido, J. (2012) A parallel solution for high resolution histological image analysis. *Comput. Methods Programs Biomed.* **108** (1), 388–401. http://doi.org/10.1016/j.cmpb.2012.03.007.

Callau, C., Lejeune, M., Korzynska, A., *et al.* (2015) Evaluation of cytokeratin-19 in breast cancer tissue samples: a comparison of automatic and manual evaluations of scanned tissue microarray cylinders. *BioMed. Eng. OnLine* **14** (2), 1–11. http://doi.org/10.1186/1475-925X-14-S2-S2.

Dodgson, N. (1997) Quadratic interpolation for image resampling. *IEEE Trans. Image Process.* **6** (9), 1322–1326. http://doi.org/10.1109/83.623195.

Hamzaoui, R. & Saupe, D. (2006) Fractal image compression. *Document and Image Compression (Signal Processing and Communications)*

(ed. by m. Barni), pp. 145–175. CRC Press, Inc., Boca Raton, FL. [ISBN 0849335566, 9780849335563]. http://doi.org/10.1201/9781420018837.

Hou, H. & Andrews, H. (1978) Cubic splines for image interpolation and digital filtering. *IEEE Trans. Acoust. Speech Signal Process.* **26** (6), 508–517. http://doi.org/10.1109/TASSP.1978.1163154.

Huynh-Thu, Q. & Ghanbari, M. (2008) Scope of validity of psnr in image/video quality assessment. *Electron. Lett.* **44** (13), 800–801. http://doi.org/10.1049/el:20080522.

Jain, A.K. (1989) *Fundamentals of Digital Image Processing*. Prentice-Hall, Inc., Upper Saddle River, NJ.

Kay, M.S. (1949). The television test pattern. *Radio & Tel. News* **41** (1), 38–39, 135–136.

Keys, R. (1981). Cubic convolution interpolation for digital image processing. *IEEE Trans.Acoust. Speech Signal Process.* **29** (6), 1153–1160. http://doi.org/10.1109/TASSP.1981.1163711.

Korzynska, A., Neuman, U., Lopez, C., Lejeun, M. & Bosch, R. (2010) The method of immunohistochemical images standardization. *Image Processing and Communications Challenges 2, Volume 84 of Advances in Intelligent and Soft Computing*, (ed. by R.S. Choras), pp. 213–221. Springer, Berlin/Heidelberg. http://doi.org/10.1007/978-3-642-16295-4_24.

Korzynska, A., Roszkowiak, L., Lopez, C., Bosch, R., Witkowski, L. & Lejeune, M. (2013) Validation of various adaptive threshold methods of segmentation applied to follicular lymphoma digital images stained with 3,3'-diaminobenzidine&haematoxylin. *Diagnost. Pathol.* **8** (1), 1–21. http://doi.org/10.1186/1746-1596-8-48.

Korzynska, A., Roszkowiak, L., Pijanowska, D., Kozlowski, W. & Markiewicz, T. (2014) The influence of the microscope lamp filament colour temperature on the process of digital images of histological slides acquisition standardization. *Diagnost. Pathol.* **9** (Suppl. 1), 1–8. http://doi.org/10.1186/1746-1596-9-S1-S13.

Lehmann, T., Gonner, C. & Spitzer, K. (1999) Survey: interpolation methods in medical image processing. *IEEE Trans. Med. Imag.* **18** (11), 1049–1075. http://doi.org/10.1109/42.816070.

Lopez, C., Callau, C., Bosch, R., *et al.* (2014) Development of automated quantification methodologies of immunohistochemical markers to determine patterns of immune response in breast cancer: a retrospective cohort study. *BMJ Open* **4** (8), e005643. http://doi.org/10.1136/bmjopen-2014-005643.

Markiewicz, T. (2011) Using matlab software with tomcat server and java platform for remote image analysis in pathology. *Diagnost. Pathol.* **6**, 1–7. http://doi.org/10.1186/1746-1596-6-S1-S18.

Markiewicz, T. (2016) Medical image analysis platform, Available at https://miap.wim.mil.pl. (last accessed date June 2016).

Markiewicz, T., Wisniewski, P., Osowski, S., Patera, J., Kozlowski, W. & Koktysz, R. (2009) Comparative analysis of methods for accurate recognition of cells through nuclei staining of ki-67 in neuroblastoma and estrogen/progesterone status staining in breast cancer. *Analyt. Quantitat. Cytol. Histol.* **31** (1), 49–62.

Meijering, E. (2002) A chronology of interpolation: from ancient astronomy to modern signal and image processing. *Proc. IEEE* **90** (3), 319–342. http://doi.org/10.1109/5.993400.

Meijering, E.H., Niessen, W.J. & Viergever, M.A. (2001). Quantitative evaluation of convolution-based methods for medical image interpolation. *Med. Image Anal.* **5** (2), 111–126. http://doi.org/10.1016/S1361-8415(00)00040-2.

Meijering, E.H.W., Niessen, W.J., Pluim, J.P.W. & Viergever, M.A. (1999) Quantitative comparison of sinc-approximating kernels for medical image interpolation. *In Proceedings of Medical Image Computing and Computer-Assisted Intervention – MICCAI'99: Second International Conference, pp. 210–217. Springer, Berlin Heidelberg. [Cambridge, UK, 19–22 September, 1999]*. http://doi.org/10.1007/10704282_23.

Mitchell, D.P. & Netravali, A.N. (1988) Reconstruction filters in computer-graphics. *SIGGRAPH Comput. Graph.* **22** (4), 221–228. http://doi.org/10.1145/378456.378514.

Neuman, U., Korzynska, A., Lopez, C. & Lejeune, M. (2010) Segmentation of stained lymphoma tissue section images. In *Information Technologies in Biomedicine* (eds. by E. Pietka & J. Kawa), Volume 2, pp. 101–113. Springer, Berlin, Heidelberg. http://doi.org/10.1007/978-3-642-13105-9_11.

Neuman, U., Korzynska, A., Lopez, C., Lejeune, M., Roszkowiak, L. & Bosch, R. (2013) Equalisation of archival microscopic images from immunohistochemically stained tissue sections. *Biocybernet. Biomed. Eng.* **33** (1), 63–76. http://doi.org/10.1016/S0208-5216(13)70056-1.

Rojo, M., Bueno, G. & Slodkowska, J. (2010) Review of imaging solutions for integrated quantitative immunohistochemistry in the pathology daily practice. *Folia Histochemica et Cytobiologica* **47** (3), 349–354. http://doi.org/10.2478/v10042-008-0114-4.

Roszkowiak, L., Korzynska, A., Lejeune, M., Bosch, R. & Lopez, C. (2016) Improvements to segmentation method of a stained lymphoma tissue section images. In *Proceedings of the 9th International Conference on Computer Recognition Systems CORES 2015* (ed. by Janusz Kacprzyk), pp. 609–617. Springer International Publishing. http://doi.org/10.1007/978-3-319-26227-7_57.

Rouse, D. & Hemami, S. (2008) Understanding and simplifying the structural similarity metric. In *15th IEEE International Conference on Image Processing, 2008. ICIP 2008*, pp. 1188–1191. http://doi.org/10.1109/ICIP.2008.4711973.

Rowland, S.W. (1979) Image reconstruction from projections: implementation and applications. *Computer Implementation of Image Reconstruction Formulas* (ed. by G. T. Herman), pp. 9–70. Springer-Verlag, Berlin, Germany. http://doi.org/10.1007/3-540-09417-2_2.

Schafer, R. & Rabiner, L. (1973) A digital signal processing approach to interpolation. *Proc. IEEE* **61** (6), 692–702. http://doi.org/10.1109/PROC.1973.9150.

Scheiber, E. (2011) On the interpolation trigonometric polynomial with an arbitrary even number of nodes. In *2011 13th International Symposium on Symbolic and Numeric Algorithms for Scientific Computing*, pp. 71–74, IEEE Computer Society, Los Alamitos, CA. http://doi.org/10.1109/SYNASC.2011.13.

Sellaro, T., Filkins, R., Hoffman, C., Fine, J., Ho, J., Parwani, A., Pantanowitz, L. & Montalto, M. (2013) Relationship between magnification and resolution in digital pathology systems. *J. Pathol. Informat.* **4** (1), 1–5. http://doi.org/10.4103/2153-3539.116866.

Slodkowska, J., Markiewicz, T., Grala, B., Kozlowski, W., Papierz, W., Pleskacz, K. & Murawski, P. (2011) Accuracy of a remote quantitative image analysis in the whole slide images. *Diagnost. Pathol.* **6** (1), 1–5. http://doi.org/10.1186/1746-1596-6-S1-S20.

Spitzbart, A. (1960) A generalization of hermite's interpolation formula. *Am. Math. Month.* **67** (1), 42–46. http://doi.org/10.2307/2308924.

Swiderska, Z., Korzynska, A., Markiewicz, T., Lorent, M., Zak, J., Wesolowska, A., Roszkowiak, L., Slodkowska, J. & Grala, B. (2015) Comparison of the manual, semiautomatic, and automatic selection and leveling of hot spots in whole slide images for ki-67 quantification in meningiomas. *Anal. Cell Pathol.* **2015**, 1–15. http://doi.org/10.1155/2015/498746.

Thevenaz, P., Blu, T. & Unser, M. (2000) Image interpolation and resampling. *Handbook of Medical Imaging, Processing and Analysis* (ed. by I. Bankman), pp. 393–420. Academic Press, San Diego CA.

Twigg, C. (2003) Catmull-rom splines. *Computer* **41** (6), 4–6.

Unser, M., Aldroubi, A. & Eden, M. (1991) Fast b-spline transforms for continuous image representation and interpolation. *IEEE Trans. Pattern Anal. Machine Intell.* **13** (3), 277–285. http://doi.org/10.1109/34.75515.

Wang, Z., Bovik, A., Sheikh, H. & Simoncelli, E. (2004) Image quality assessment: from error visibility to structural similarity. *IEEE Trans. Image Process.* **13** (4), 600–612. http://doi.org/10.1109/TIP.2003.819861.

Welstead, S.T. (1999) *Fractal and Wavelet Image Compression Techniques*, Volume 40. SPIE Press, Bellingham, WA, USA.

Yuksel, C., Schaefer, S. & Keyser, J. (2009) On the parameterization of catmull-rom curves. In *2009 SIAM/ACM Joint Conference on Geometric and Physical Modeling*, SPM '09, pp. 47–53. ACM, New York, NY. http://doi.org/10.1145/1629255.1629262.